

ESTIMATING THE COLOR PALETTE OF ORTELIUS' ATLAS: A CASE STUDY OF HYPERSPECTRAL IMAGING FOR RAPID PIGMENT SCREENING

Hilda Deborah¹, Chiara Palandri², Giulia Oretti²

¹Department of Computer Science, Norwegian University of Science & Technology

²Department of Collections and Research, National Library of Norway

ABSTRACT

The map collection, *Kartsenteret*, of the National Library of Norway is conducting a pilot study of its collection of approximately 150,000 maps. This collection covers a 500-year map and color history. Aiming to study the colors of the historical maps and their relationship, hyperspectral imaging is chosen as the first step where rapid screening and testing of the potential pigments or colorants can be carried out. The estimation is performed by means of spectral distance or similarity measures, tested against an available public dataset of pigments which also contains historical pigments. Finally, we are able to provide a list of pigments as estimated by a spectral distance function, to be validated in further analytical tests.

Index Terms— Pigment matching, distance function, similarity, hyperspectral imaging.

1. INTRODUCTION

The analysis and identification of pigments and colorants is perhaps the most popular use of hyperspectral imaging (HSI) for cultural heritage applications [1–3]. Here, mostly the visible and infrared (NIR or SWIR) spectral region are of focus. The basic assumption is that materials, especially colorants, carry characteristics and discriminative information in these ranges, more than the traditional color imaging would. However, as also pointed out in Ref. [4], this assumption only holds in very specific cases [5] and can be misleading when used for identifying pigments or the constituents of a paint layer. To do so, HSI cannot act alone and further analytical methods must be carried out.

While HSI is not to replace analytical methods, it remains a powerful complementary method and analysis that allows the non-invasive and rapid scanning of the entire surface of an object. On the other hand, the result of chemical analysis are only representative of limited area [4] and should not be generalized into the whole spatial extent of the surface. In this regard, the use of HSI is relevant as the first scientific screening or study of a larger collection of, e.g., ancient manuscripts or maps. This is especially true for fragile and brittle objects where their handling and removal from the storage or display solution can be prohibitive to the study of the materials [6].

The focus of this study is the use of HSI in the context of the map collection at the National Library of Norway. Its map collection, *Kartsenteret*, contains approximately 150,000 maps and covers a 500-year map history, and an equally long color history. This work is part of a pilot project towards the study of the colors of the historical maps and their relationship. In this direction, a corpus of representative atlases and loose maps was selected. It contains 11 copies of the Abraham Ortelius *Theatrum Orbis Terrarum* [7], of different editions from 1570 to 1641, 25 copies of what is called of "Mini-Ortelius" (shortened versions of Ortelius' atlas in small formats published by several different publishers), and approximately 45 loose maps from the Ortelius Atlas depicting: 36 Scandinavia, 5 Iceland, 3 Denmark and 1 one world map. One of the maps from Ortelius' Atlas showing Scandinavia was selected to establish the analytical methodology on color analysis, which will be analysed throughout this paper.


To perform the pigment estimation of the map under study, several spectral distance or similarity measures are investigated. Specifically, we only focus on those that put importance in shape differences and suppresses the impact of magnitude or intensity of the spectra, e.g., spectral angle [8], goodness-of-fit coefficient [9], and the shape component of Kullback Leibler pseudo-divergence [10]. This choice is made because the characteristic signature of a pigment is often in the peaks or inflections of its spectral reflectance signals [4, 10]. Finally, a list of suggested pigments are provided at the end of this work.

2. MATERIALS

2.1. The case study map

The map under study is as shown below. Both mechanical and chemical-physical damages are present on the support in the areas corresponding to the green color, in the form of browning with migration on the adjacent areas and the verso, and fracturing of the embrittled paper support, which are consistent with the use of copper acetate pigments (Verdigris). Observed at 40x magnification, the red pigment and the green pigment used in the outer line reveal cracking and loss. More of its detailed information are provided in Table 1.

Table 1: Identification and information regarding the selected Ortelius' map for this work.

	
Title	SEP/TEN/TRI/ONA/LIVM RE/GIONVM/DESCRIP.
Edition	1588
Place	Antwerp
Scale	1:10,000,000
Technique	Engraving (burin)
Colors	Hand coloring
Notes	From a Spanish edition of the Theatrum Orbis Terrarum (Theatro de la Tierra Universal). Edition published by Christophe Plantin (1520-1589), considered to be the most important printer and publisher in the Netherlands in the second half of the 16th century.

2.2. Hyperspectral image target

A portable hyperspectral scanner Specim IQ was used to acquire areas of interest from the map, focusing on capturing areas with different colors. A total of six hyperspectral images are used in this study, each with 204 spectral bands covering the range of 397.32 to 1003.58 nanometers (nm), in 3.09 nm intervals. These images are 512×512 pixels. Examples of the images can be observed in Fig. 1. Note that the hyperspectral images are processed in terms of spectral reflectance.

At the time of this study, none of the pixels in the target images have any corresponding ground truth information coming from analytical studies. Thus, for each image, several pixels are manually sampled to represent the different colors present in the map. These then become the target pixels for the pigment estimation. Spectral reflectance corresponding to the sampled pixels in Fig. 1 are provided in Fig. 2. Both the colors shown in Fig. 1 and 2 are generated from the hyperspectral images by means of a color transformation that

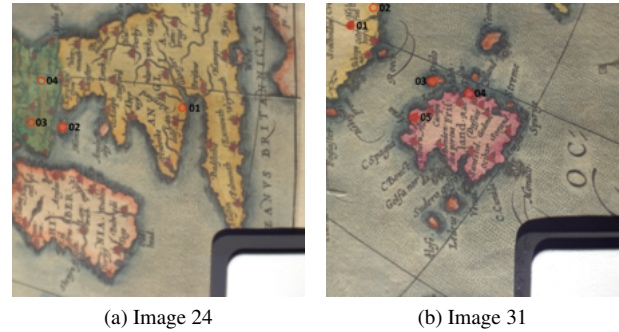


Fig. 1: Example of the captured hyperspectral images, showing also the calibration target in the lower right corner. Red circles in each image show the approximate area where spectra are sampled for pigment estimation. These images are generated from its hyperspectral image using a color transformation with CIE Color Matching Function 2°Standard Observer and D65 illumination.

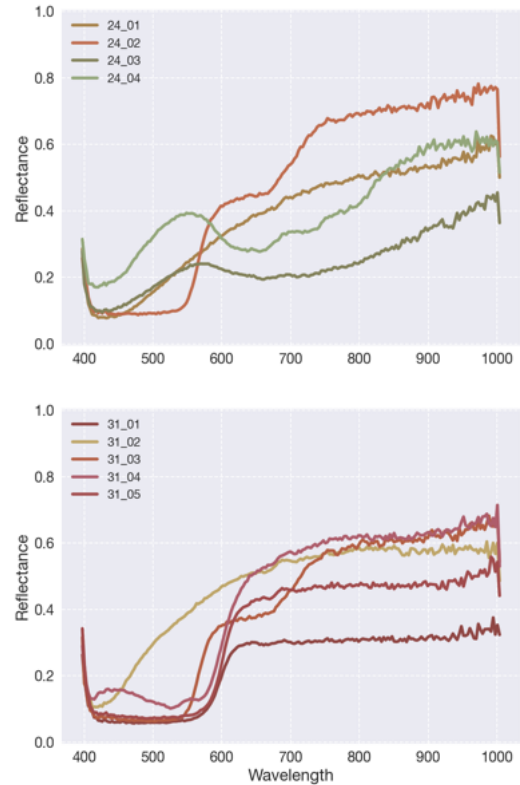


Fig. 2: Spectra corresponding to the samples shown in Fig. 1.

employs the CIE Color Matching Function 2°Standard Observer and D65 standard illuminant. Unless stated otherwise, color visualisation in the rest of this paper is produced the same way. This color transformation simulates how the pigment would be perceived by normal vision under daylight at noon and is a standard procedure laid out in colorimetry.

2.3. Spectral library

A spectral library of Kremer pigments are available online [11] and it is the one used in this work. Its spectral dimension is, however, different from the hyperspectral image target, i.e., 186 bands at 3.26 nm intervals, captured between the range 405.37 to 995.83 nm. This means that before using both target image and spectral library, data interpolation must be carried out and it will be explained in the next section. The spectral library contains signatures of 327 pure pigments, where for each pigment four signatures corresponding to its different shades are also available. As an illustration, green earth pigments found in the library are plotted in Fig. 3.

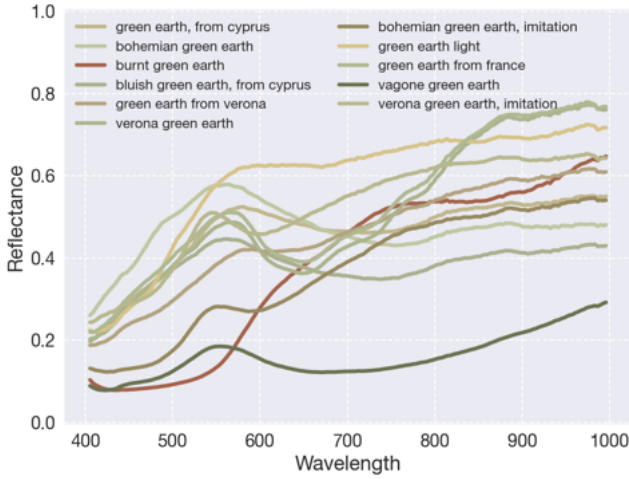


Fig. 3: Green earth pigments found in the spectral library used in this work.

3. EXPERIMENTAL SETUP

To estimate the color palette of Ortelius' atlas, pigment matching to an available spectral library is conducted. Specifically in this work, the workflow is as depicted in Fig. 4.

3.1. Spectral interpolation

As briefly mentioned previously, the target spectral images and pixels do not have the same dimension as the spectral library being used. Since the target image has a finer spectral interval of 3.09 nm, it was decided that the spectral library is the one being interpolated to the wavelengths of the target image. A one-dimensional linear interpolation was chosen, assuming a monotonically increasing sample points. This assumption is met since we consider a spectrum to be a function of wavelength, where the wavelength is ordered in increasing manner (as opposed to, e.g., vector where the order of the wavelength does not matter).

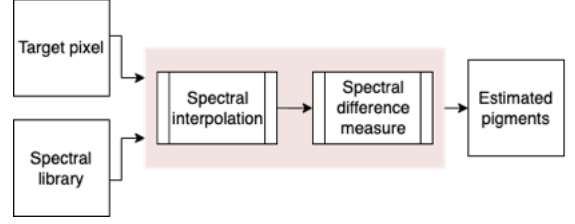


Fig. 4: Workflow of the pigment estimation of the Ortelius' map. The spectral interpolation step is needed due to differences in the spectral dimensions of the target pixel and the spectral library.

3.2. Spectral difference measures

Since the characteristic signature of pigments are more often found in the peak and inflection of their spectra, only difference measures that consider the shape or angle of a spectrum is considered. Note that here the term difference is to encompass both distance and similarity measures. The chosen measures are **spectral angle** (SAM) [8]:

$$\text{SAM}(S_1, S_2) = \cos^{-1}(\text{sim}_{\cos}(S_1, S_2)),$$

which is based on the calculation of cosine similarity between two spectra S_1 and S_2 :

$$\text{sim}_{\cos}(S_1, S_2) = \frac{\int_{\lambda} (s_1(\lambda) \cdot s_2(\lambda)) d\lambda}{(\int_{\lambda} s_1(\lambda)^2 d\lambda)^{\frac{1}{2}} (\int_{\lambda} s_2(\lambda)^2 d\lambda)^{\frac{1}{2}}}.$$

The **goodness-of-fit coefficient** (GFC) [9] is developed based on Schwartz's inequality. In the Euclidean space, it is essentially the cosine distance:

$$\text{GFC}(S_1, S_2) = \frac{|\int_{\lambda} s_1(\lambda) \cdot s_2(\lambda) d\lambda|}{\sqrt{|\int_{\lambda} s_1(\lambda)^2 d\lambda|} \sqrt{|\int_{\lambda} s_2(\lambda)^2 d\lambda|}}.$$

The last measure being considered is the shape component of the **Kullback-Leibler pseudo-divergence** (sKLDP) [10], which was written based on the Kullback-Leibler divergence:

$$\text{KL}(\bar{S}_1, \bar{S}_2) = \int_{\lambda_{\min}}^{\lambda_{\max}} \bar{S}_1(\lambda) \cdot \ln \frac{\bar{S}_1(\lambda)}{\bar{S}_2(\lambda)} d\lambda,$$

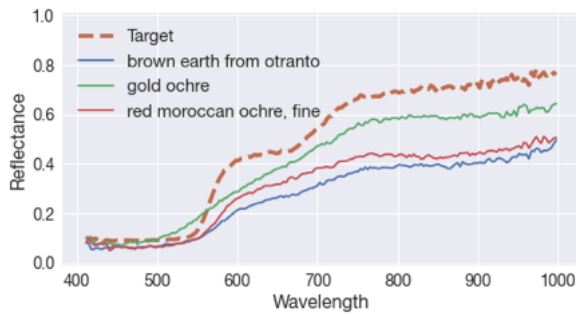
where it considers the normalized input or spectra \bar{S} . This is because KL divergence is a measure between two probability density functions (PDFs), thus a spectrum must be converted to a PDF beforehand. Finally the expression for sKLDP is:

$$\text{sKLDP}(S_1, S_2) = k_1 \cdot \text{KL}(\bar{S}_1, \bar{S}_2) + k_2 \cdot \text{KL}(\bar{S}_2, \bar{S}_1),$$

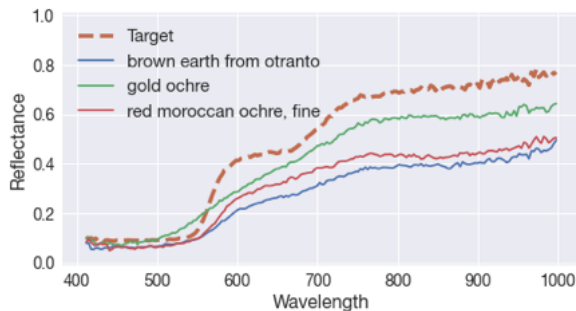
where k_i is the total intensity or energy of spectrum S_i computed by means of its integral.

4. RESULTS AND DISCUSSION

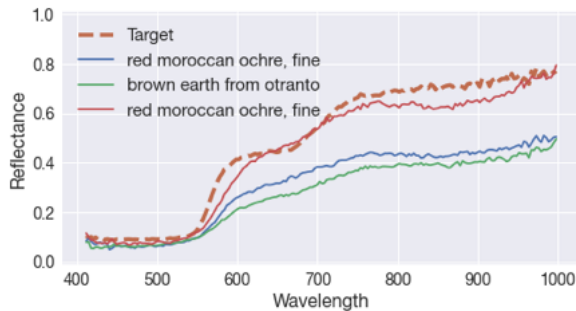
Starting with the samples or target pixels taken from image 24, see spectra in Fig. 2, where we have one red, one yellow or brown, and two green pigments that are unknown. For the two green samples 24_03 and 24_04, all SAM, GFC, and sKLPD agree that the most similar are vagone green earth and verona green earth, respectively. Different results are obtained by SAM, GFC, and sKLPD for the reddish sample 24_02, see Fig. 5 showing the three best pigment matches. Note that in this figure, only the color of the target spectrum is generated using a color transformation (or is in its true color). The pigment matches are plotted in arbitrary colormap, i.e.,



(a) SAM



(b) GFC



(c) sKLPD

Fig. 5: Three best pigment matches determined by SAM, GFC, and sKLPD. Note that only the target spectrum is rendered in its true color, while the rest are colored arbitrarily.

blue, green, red. Looking at the identical results of SAM and GFC, we see that a gold ochre pigment is suggested as the second best match to the target spectrum. The spectrum of gold ochre only has one step shape peaking at around 750 nm. Meanwhile, the target spectrum and two other suggested matches, have another step shape with the peak at around 600 nm. This suggests that SAM and GFC is not sufficient for pigment analysis application, since it is less sensitive to information in peak and inflection points, less so than sKLPD. While similarly suggesting red moroccan ochre and brown earth from otranto, sKLPD does not suggest gold ochre and, instead, found another shade of the red moroccan ochre to be a match. Finally, sKLPD suggested that the last sample from the same image, i.e., 24_01, to be an indian yellow imitation. From this point, the suggestion from SAM and GFC will not be considered due to the aforementioned reason.

For the samples taken from image 31, see Fig. 2, the best matches for 31_01 to 31_05 are vermilion, naples yellow-reddish, red moroccan ochre, CPT-red, and studio red-helio. They were suggested albeit with varying difference values to their corresponding target spectrum. Note that the values of sKLPD ranges between $[0, +\infty]$, with better pigment matches having values closer to 0. The lowest sKLPD value is found in the match for 31_01, i.e., vermilion, with a difference value

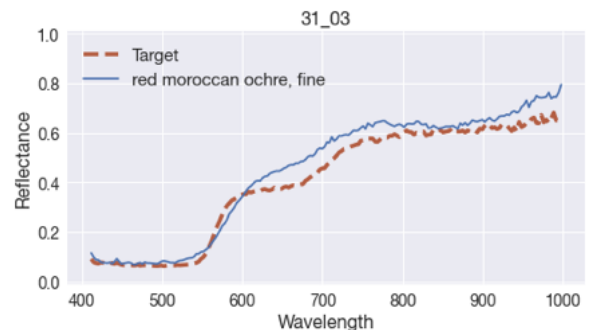
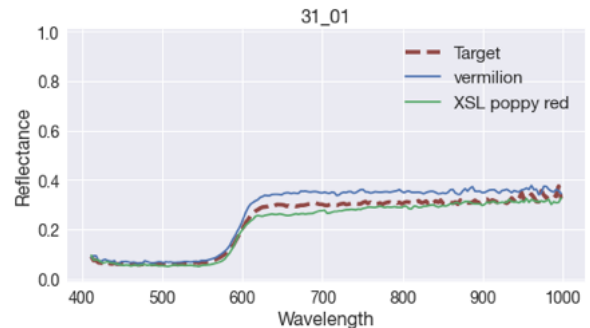


Fig. 6: Samples from Image 31 (Fig. 1) with the lowest and highest difference values to their respective matching pigments. Sample 31_01 is found to be a very close match to vermilion, with score 0.2. The match for 31_03 is suggested with less confidence, that is with a difference value of 1.31.

0.2. In Fig. 6, we can see that vermilion and the target are almost identical in their spectral shape, with slight intensity differences after 600 nm. The highest difference is found in the match for sample 31_03 with a value 1.31, which reflects a lower confidence in finding a good match, especially in the location of the peak and inflection points.

Learning from the above result, we then provide a threshold for suggesting a pigment match, i.e., $sKLPD \leq 1.0$. Using this threshold, the rest of the samples taken from the other available images are matched to the spectral library. The completed estimation of pigments found in the map of study is provided in Table 2. Only the best match among the suggested ones with difference values less than the threshold are mentioned in this table. This also means that not all of the samples found a match in the library, e.g., blue samples. For such, further investigation is needed by either expanding the spectral library or considering an unmixing approach.

Table 2: The result of pigment estimation by matching samples taken from the hyperspectral image of the selected Ortelius’ map to the spectral library made of Kremer pigments.

Yellow, orange	Indian yellow imitation French ochre HAVANE Amberg yellow Isoindolol orange Naples yellow, reddish Irgazine orange DPP RTR
Green	Vagone green earth Verona green earth
Red, pink	Red moroccan ochre Permanent red A Dark burnt sienna Vermilion CPT - red Studio red, helio

5. CONCLUSION

This work has been a part of a pilot project aiming at studying the collection of approximately 150,000 maps at the National Library of Norway. Hyperspectral imaging (HSI) has been employed to provide an estimation of what pigments or colorants may exist in the colorant. Compared to the more traditional way of identifying the pigments by means of analytical methods, HSI allows rapid scanning and estimation of pigments. Furthermore, HSI does not require physically sampling materials and is able to analyse the entire spatial extent of an object, a capability usually not offered by analytical methods. However, it is important to remember that HSI does not provide a conclusive identification of pigments, and must always be followed by further analytical tests. The two approaches are highly complementary in conducting a

comprehensive study for, especially, a larger collection of objects. For this study, further analytical examinations will be performed for the pigments in the map collection.

6. REFERENCES

- [1] C. Balas, G. Epitropou, et al., “Hyperspectral imaging and spectral classification for pigment identification and mapping in paintings by El Greco and his workshop,” *Multimedia Tools and Applications*, vol. 77, no. 8, pp. 9737–9751, Apr. 2018.
- [2] T. Kleynhans, D. W. Messinger, et al., “Low-Cost Multispectral System Design for Pigment Analysis in Works of Art,” *Sensors*, vol. 21, no. 15, pp. 5138, 2021.
- [3] M. González-Cabrera, K. Wieland, et al., “Multisensor hyperspectral imaging approach for the microchemical analysis of ultramarine blue pigments,” *Scientific Reports*, vol. 12, no. 1, pp. 707, 2022.
- [4] L. Pronti, A. Pelagotti, et al., “Intrinsic limits of reflectance spectroscopy in identifying pigments in paint layers,” *IOP Conference Series: Materials Science and Engineering*, vol. 364, pp. 012061, June 2018.
- [5] H. Deborah, M. O. Ulfarsson, and J. Sigurdsson, “Fully Constrained Least Squares Linear Spectral Unmixing of The Scream (Verso, 1893),” in *11th Workshop on Hyperspectral Imaging and Signal Processing: Evolution in Remote Sensing (WHISPERS)*. 2021, pp. 1–5, IEEE.
- [6] H. Deborah and A. Kostomitsopoulou Marketou, “Spectral Imaging of Ink Behind Glass: A Preliminary Investigation of the Colorimetric Shift,” in *Archiving Conference*. 2023, vol. 20, pp. 204–208, IS&T.
- [7] M. P. R. Van Den Broecke, P. C. J. Van Der Krogt, and P. H. Meurer, Eds., *Abraham Ortelius and the First Atlas: Essays Commemorating the Quadricentennial of His Death, 1598-1998*, H & S, Houten, 1998.
- [8] F. A. Kruse, A. B. Lefkoff, et al., “The spectral image processing system (SIPS)—interactive visualization and analysis of imaging spectrometer data,” *Remote Sensing of Environment*, vol. 44, no. 2-3, pp. 145–163, 1993.
- [9] J. Hernández-Andrés, J. Romero, et al., “Color and spectral analysis of daylight in southern Europe,” *Journal of the Optical Society of America A*, vol. 18, no. 6, pp. 1325, 2001.
- [10] H. Deborah, *Towards Spectral Mathematical Morphology*, Ph.D. thesis, NTNU, Université de Poitiers, 2016.
- [11] H. Deborah, “Hyperspectral Pigment Dataset,” in *12th Workshop on Hyperspectral Imaging and Signal Processing: Evolution in Remote Sensing (WHISPERS)*. 2022, pp. 1–5, IEEE.